AFRL-RY-WP-TP-2010-1187

HIGH ELECTRON MOBILITY TRANSITSORS (HEMT)
Selected Papers

Lin Zhou, David A. Cullen, David J. Smith, Martha R. McCartney, F.A. Marin, N. Faralli, D.K. Ferry, S.M. Goodnick, and M. Saraniti

Arizona State University

Anas Mouti, M. Gonschorek, E. Feltin, J.F. Carlin, and N. Grandjean

Ecole Polytechnique Federale de Lausanne (EPFL)

J. Leach and H. Morkoc

Virginia Commonwealth University

P.L. Fejes

Freescale Semiconductor Inc.

JUNE 2010
Final Report

AIR FORCE RESEARCH LABORATORY
SENSORS DIRECTORATE
WRIGHT-PATTERSON AIR FORCE BASE, OH 45433-7320
AIR FORCE MATERIEL COMMAND
UNITED STATES AIR FORCE

REPORT DOCUMENTATION PAGE

Form Approved
OMB No. 0704-0188

1. REPORT DATE *(DD-MM-YY)*	2. REPORT TYPE	3. DATES COVERED *(From - To)*
June 2010	Journal Article Postprint	30 May 2008 – 30 May 2010

4. TITLE AND SUBTITLE
HIGH ELECTRON MOBILITY TRANSITSORS (HEMT)
Selected Papers

5a. CONTRACT NUMBER

5b. GRANT NUMBER
FA8650-08-C-1395

5c. PROGRAM ELEMENT NUMBER
62204F

6. AUTHOR(S)
Lin Zhou, David A. Cullen, David J. Smith, Martha R. McCartney, F.A. Marin, N. Faralli, D.K. Ferry, S.M. Goodnick, and M. Saraniti (Arizona State University)
Anas Mouti, M. Gonschorek, E. Feltin, J.F. Carlin, and N. Grandjean (Ecole Polytechnique Federale de Lausanne (EPFL))
J. Leach and H. Morkoc (Virginia Commonwealth University)
P.L. Fejes (Freescale Semiconductor Inc.)

5d. PROJECT NUMBER
2002

5e. TASK NUMBER
11

5f. WORK UNIT NUMBER
2002110B

7. PERFORMING ORGANIZATION NAME(S) AND ADDRESS(ES)
Arizona State University
Tempe, AZ 85287-8706

Ecole Polytechnique Federale de Lausanne (EPFL)

Virginia Commonwealth University

Freescale Semiconductor Inc.

8. PERFORMING ORGANIZATION REPORT NUMBER

9. SPONSORING/MONITORING AGENCY NAME(S) AND ADDRESS(ES)
Air Force Research Laboratory
Sensors Directorate
Wright-Patterson Air Force Base, OH 45433-7320
Air Force Materiel Command
United States Air Force

10. SPONSORING/MONITORING AGENCY ACRONYM(S)
AFRL/RYDD

11. SPONSORING/MONITORING AGENCY REPORT NUMBER(S)
AFRL-RY-WP-TP-2010-1187

12. DISTRIBUTION/AVAILABILITY STATEMENT
Approved for public release; distribution unlimited.

13. SUPPLEMENTARY NOTES
 This work was funded in whole or in part by Department of the Air Force Contract FA8650-08-C-1395. Published in Applied Physics Letter 94, 121909 (2009); Published in Journal of Physics: Conference Series 193 (2009) 012040; Presented at ICAM 2009, September 20 - 25, 2009, Rio de Janeiro, Brazil. This document contains color.

14. ABSTRACT
Published in support of AFRL-RY-WP-TR-2010-1178.

15. SUBJECT TERMS
microelectronics, heterostructure, holography, modeling/simulation

16. SECURITY CLASSIFICATION OF:			17. LIMITATION OF ABSTRACT:	18. NUMBER OF PAGES	19a. NAME OF RESPONSIBLE PERSON (Monitor)
a. REPORT	b. ABSTRACT	c. THIS PAGE			Ronald Schweller
Unclassified	Unclassified	Unclassified	SAR	14	19b. TELEPHONE NUMBER *(Include Area Code)* N/A

Standard Form 298 (Rev. 8-98)
Prescribed by ANSI Std. Z39-18

Polarization field mapping of $Al_{0.85}In_{0.15}N/AlN/GaN$ heterostructure

Lin Zhou,[1,a)] David A. Cullen,[1] David J. Smith,[1] Martha R. McCartney,[1] Anas Mouti,[2] M. Gonschorek,[2] E. Feltin,[2] J. F. Carlin,[2] and N. Grandjean[2]
[1]*Department of Physics, Arizona State University, Tempe, Arizona 85287, USA*
[2]*École Polytechnique Fédérale de Lausanne (EPFL), CH-1015 Lausanne, Switzerland*

(Received 4 February 2009; accepted 6 March 2009; published online 27 March 2009)

Off-axis electron holography has been used to measure the built-in potential profile across an $Al_{0.85}In_{0.15}N/AlN/GaN$ high electron mobility transistor heterostructure. Profile measurements indicated a polarization-induced electric field of 6.9 MV/cm within the AlN layer. A two-dimensional electron gas with a density of $\sim 2.1\times 10^{13}$ cm^{-2} was located in the GaN layer at ~ 0.8 nm away from the AlN/GaN interface in reasonable agreement with the reported simulations. Electron microscopy confirmed that the $Al_{0.85}In_{0.15}N$ layer was uniform and that $Al_{0.85}In_{0.15}N/AlN$ and AlN/GaN interfaces were abrupt and well defined. © *2009 American Institute of Physics*. [DOI: 10.1063/1.3108084]

The $Al_{1-x}In_xN$ material system has been proposed as the basis for fabrication of high electron mobility transistors (HEMTs).[1–5] It is predicted by Vegard's law that $Al_{0.825}In_{0.175}N$ should be lattice matched (LM) to fully relaxed GaN so that the $Al_{0.825}In_{0.175}N/GaN$ heterostructure should ideally be free of interface strain.[5] Moreover, problems associated with strain relaxation, such as defect generation and device degradation, should be alleviated.[5] Due to the spontaneous polarization difference between LM InAlN and GaN, a positive polarization charge should appear at the AlInN/GaN interface.[6] Electrons in the nearby region would tend to compensate for this polarization charge and form a two-dimensional electron gas (2DEG).[3] High performance AlInN/GaN HEMT structures grown on sapphire substrates with a 2DEG density of $\sim 2.6\times 10^{13}$ cm^{-2} have been recently reported.[4] The effect of strain on the 2DEG density at the AlInN/InN/GaN interface for AlInN barriers with different thicknesses and In concentration was also investigated.[3] However, the exact location of the 2DEG layer remains uncertain and structural analysis of such HEMTs is lacking. Here, we describe a study involving cross-sectional and plan-view transmission electron microscopy (TEM), small-probe microanalysis, as well as off-axis electron holography of the microstructure and electrostatic potential profile across an $Al_{0.85}In_{0.15}N/AlN/GaN$ HEMT structure. The position of the 2DEG has been located experimentally.

The HEMT heterostructure was grown in an AIXTRON 200/4 RF-S metalorganic vapor-phase epitaxy (MOVPE) system on a 2 in. *c*-plane sapphire substrate. Growth details can be found in Ref. 3. Samples suitable for cross-sectional and plan-view observation were prepared by mechanical wedge polishing or dimpling followed by Ar ion milling at 3.5 keV using a liquid-nitrogen cold stage to avoid any segregation artifacts. Samples for holography observations were then chemically etched in warm KOH solution. High-angle annular-dark-field (HAADF) scanning transmission electron microscopy (STEM) and energy-dispersive x-ray spectroscopy (EDXS) were conducted using a JEOL JEM-2010 FEG TEM operated at 200 keV. The focused probe size [full width at half maximum (FWHM)] for these measurements was estimated to be ~0.5 nm and the step size for analysis line scans was ~1 nm. High-resolution and diffraction-contrast imaging as well as off-axis electron holography were performed using a Philips CM200 FEG TEM equipped with an electrostatic biprism and a charge coupled device camera for quantitative image recording. A positive biprism voltage of ~105 V was used to produce holograms in high-resolution mode with the objective lens turned on.

High-resolution cross-sectional imaging revealed that the AlInN/AlN/GaN interfaces were coherent and abrupt, as shown in Fig. 1. Lower magnification TEM images (not shown here) indicated that most threading dislocations (TDs) in the upper part of the GaN layer propagated through the heterostructure to the top surface. Plan-view imaging showed that the TD density inside the HEMT was $\sim 9\times 10^{8}$ cm^{-2}.

A cross-sectional HAADF image of the $Al_{0.85}In_{0.15}N/AlN/GaN$ HEMT structure taken on the $[10\bar{1}0]$ zone axis and the corresponding EDXS line profile are shown in Fig. 2. Abrupt $Al_{0.85}In_{0.15}N/AlN$ and AlN/GaN interfaces are observed. The uniform contrast in the AlInN indicates that there is no phase separation in this layer. The thicknesses of the AlInN and AlN layers measured from the STEM images are 13 and 1.3 nm, respectively.

Off-axis electron holography provides quantitative access to phase shifts experienced by the incident electron

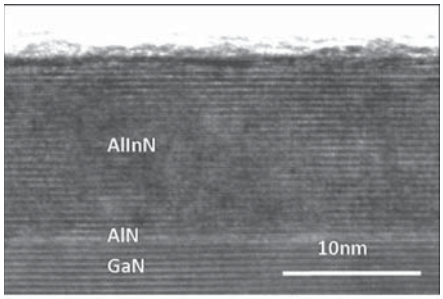

FIG. 1. Cross-sectional high-resolution TEM image recorded in $[11\bar{2}0]$ zone axis projection showing that AlInN/AlN and AlN/GaN interfaces are well defined.

a)Electronic mail: linzhou@asu.edu.

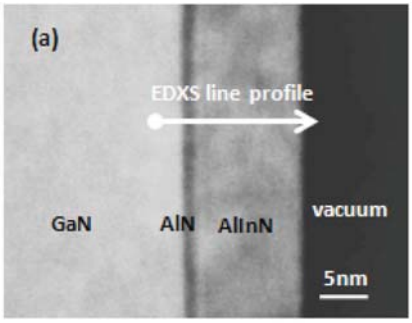

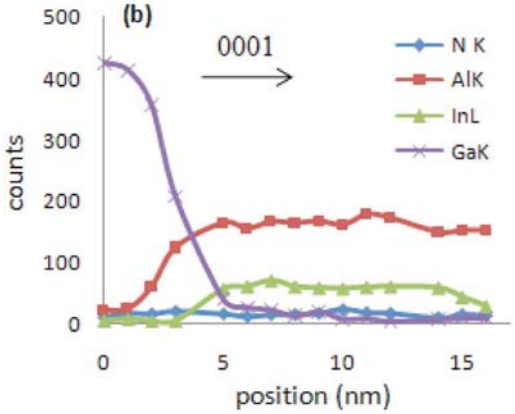

FIG. 2. (Color online) (a) HAADF STEM image of the HEMT structure; (b) EDXS line profile across the interface from the region indicated in (a).

wave front due to interactions with the electrostatic and magnetic potential of the sample.[7] The technique was used here to map electrostatic potential profiles across the $Al_{0.85}In_{0.15}N/AlN/GaN$ HEMT structure. When a TEM sample is not in a strongly diffracting condition and has a uniform potential through its projected thickness, then the relationship between the holographic phase shift Φ and electrostatic potential V is simply given by

$$\Phi = C_E V t, \tag{1}$$

where C_E is an energy-dependent constant (0.007 28 rad/V nm for 200 keV electrons) and t is the sample thickness.[7] Since the AlInN layer was very close to vacuum and thin TEM samples close to vacuum may be easily bent or damaged during sample preparation, holograms were taken from relatively thick regions to minimize these effects. Moreover, holographic analysis concentrated on the $Al_{0.85}In_{0.15}N/AlN/GaN$ interface area away from the sample edge.

Figures 3(a) and 3(b) show the phase and amplitude images, respectively, from the reconstructed hologram of the $Al_{0.85}In_{0.15}N/AlN/GaN$ HEMT. The phase in vacuum was set to zero. A line profile through the phase image across the heterostructure averaged over 15 nm along the [0001] growth direction is shown in Fig. 4. The sample thickness (228 nm) was extracted from the amplitude of the hologram

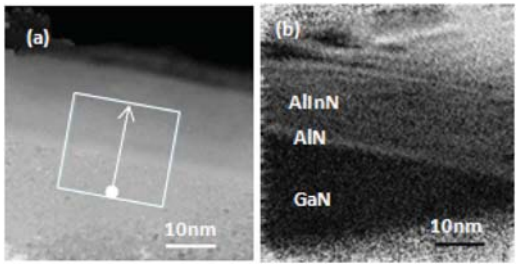

FIG. 3. (Color online) (a) Phase and (b) amplitude images from reconstructed hologram of the HEMT structure.

by taking the inelastic mean free path for GaN as 61 nm.[8] Line profiles from the thickness image confirmed uniform thickness in the area analyzed.

Figure 5 shows the potential profile across the $Al_{0.85}In_{0.15}N/AlN/GaN$ heterostructure calculated using Eq. (1). This yields a value of ~13.4 V for the mean-inner potential of GaN in good agreement with the published values.[9–11] A linear drop in potential inside the AlN layer consistent with an electric field inside the AlN layer (E^{AlN}) is also visible. E^{AlN} is generated by polarization charges located at the AlInN/AlN (negative charges) and AlN/GaN (positive charges) interfaces.[5] Assuming that E^{AlN} is constant across the AlN layer, then its value can be obtained by fitting the slope of the potential in that region $[E^{AlN}=-d(V_0^{AlN}+V_E^{AlN})/dx=-d(V_E^{AlN})/dx$ from positions 7.18 to 9.45 nm]. The result of ~6.9 MV/cm is consistent with the reported theoretical calculations.[3,6] However, the expected drop in mean inner potential at the AlN/GaN and InAlN/AlN interfaces was not visible, which is consistent with other observations.[10]

The positive curvature of potential near the AlN/GaN interface region indicates the existence of a 2DEG.[10] This 2DEG was quantified using the following steps. First, numerical Gaussian fitting from the experimental data was performed from positions 2.8 to 7.0 nm to smooth the experimental data. The second derivative of the fitted profile was calculated and the electron density (n) was then obtained using $n=-\varepsilon_0\varepsilon_r d^2V/dx^2$ (for GaN ε_r: 10.5). Finally, the 2DEG density was calculated by integrating n along the

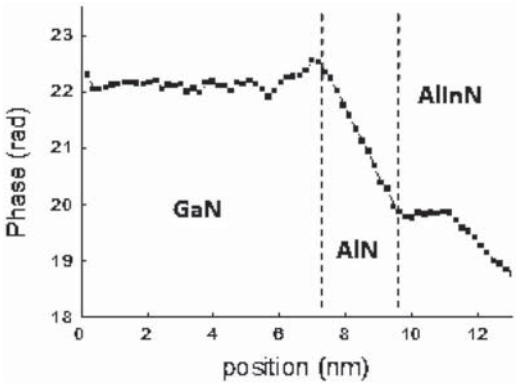

FIG. 4. Phase profile across the AlInN/AlN/GaN interface.

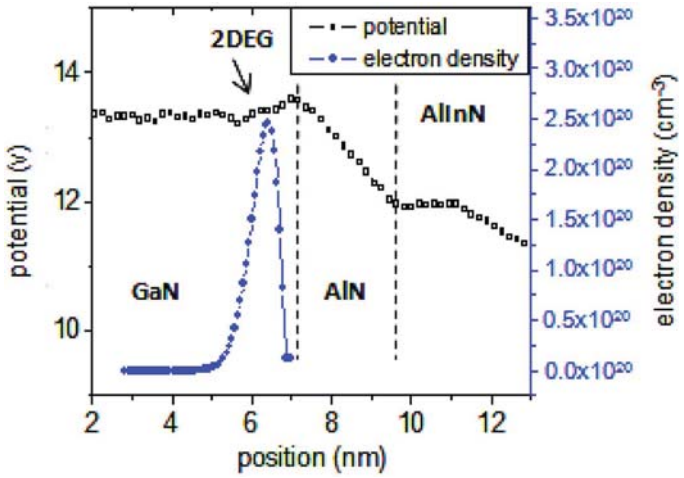

FIG. 5. (Color online) Potential profile (open squares) and electron distribution (filled circles) across the AlInN/AlN/GaN interface.

[0001] direction from positions 2.8 to 7.0 nm. A Gaussian electron distribution around the AlN/GaN interface was revealed, as shown in Fig. 5. The peak electron density in the GaN layer of 2.45×10^{20} cm^{-3} was located at about ~0.8 nm away from the AlN/GaN chemical interface and the integrated 2DEG density was $\sim2.1\times10^{13}$ cm^{-2}.

A comparison between electron holography measurements and simulated values is shown in Table I. The measured E^{AlN} and 2DEG density are consistent with theoretical simulations. The slightly smaller experimental value could be due to a screening effect caused by charges at the interfaces. Electrically dead layers at the TEM sample surface may also cause some slightly underestimation. However, the measured maximum electron density at the interface is higher than the simulated value. One possible explanation is that the electrons are better confined than in the simulated curve (narrower FWHM).

In conclusion, $Al_{0.85}In_{0.15}N/AlN/GaN$ HEMT heterostructure with well defined interfaces have been grown on *c*-plane sapphire substrates using MOVPE. The measurement of electrostatic potential profiles across the heterostructure by off-axis electron holography showed an electric field of ~6.9 MV/cm within the AlN layer. A 2DEG with a density of $\sim2.1\times10^{13}$ cm^{-2} was located in the GaN at ~0.8 nm away from the AlN/GaN interface.

TABLE I. Comparison of simulated and experimental values of the electric field, 2DEG density, and location across the HEMT structure.

	Simulation	Hall effect	Off-axis electron holography
E^{AlN} (MV/cm)	7.5[a]		6.9
2DEG density ($\times10^{13}$ cm^{-2})	2.5[a]	2.53[a]	2.1
Maximum charge density ($\times10^{20}$ cm^{-3})	1.25[a]		2.45
Distance of 2DEG from AlN/GaN interface (nm)	~0.63 [b]		~0.8

[a]Reference 3.
[b]Reference 2.

This work was supported by a contract from Wright Patterson Air Force Base (Monitor: C. Bozada) and the Swiss National Science Foundation (Contract No. 200021-107642/1). We acknowledge the use of facilities at John M. Cowley Center for High Resolution Electron Microscopy at Arizona State University.

[1]J. Kuzmík, IEEE Electron Device Lett. **22**, 510 (2001).
[2]R. Butté, J.-F. Carlin, E. Feltin, M. Gonschorek, S. Nicolay, G. Christmann, D. Simeonov, A. Castiglia, J. Dorsaz, H. J. Buehlmann, S. Christopoulos, G. Baldassarri Höger von Högersthal, A. J. D. Grundy, M. Mosca, C. Pinquier, M. A. Py, F. Demangeot, J. Frandon, P. G. Lagoudakis, J. J. Baumberg, and N. Grandjean, J. Phys. D **40**, 6328 (2007).
[3]M. Gonschorek, J.-F. Carlin, E. Feltin, M. A. Py, N. Grandjean, V. Darakchieva, B. Monemar, M. Lorenz, and G. Ramm, J. Appl. Phys. **103**, 093714 (2008).
[4]M. Gonschorek, J.-F. Carlin, E. Feltin, M. A. Py, and N. Grandjean, Appl. Phys. Lett. **89**, 062106 (2006).
[5]L. Zhou, D. J. Smith, M. R. McCartney, D. S. Katzer, and D. F. Storm, Appl. Phys. Lett. **90**, 081917 (2007).
[6]F. Bernardini, V. Fiorentini, and D. Vanderbilt, Phys. Rev. B **56**, R10024 (1997).
[7]M. R. McCartney and D. J. Smith, Annu. Rev. Mater. Res. **37**, 729 (2007).
[8]Z. H. Wu, M. Stevens, F. A. Ponce, W. Lee, J. H. Ryou, D. Yoo, and R. D. Dupuis, Appl. Phys. Lett. **90**, 032101 (2007).
[9]M. Gajdardziska-Josifovska and A. H. Carim, in *Introduction to Electron Holography*, edited by E. Volkl, L. Allard, and D. Joy (Plenum, New York, 1999), p. 267.
[10]M. R. McCartney, F. A. Ponce, J. Cai, and D. P. Bour, Appl. Phys. Lett. **76**, 3055 (2000).
[11]S. Tanaka, A. Naito, Y. Honda, N. Sawaki, and M. Ichihashi, J. Electron Microsc. **56**, 37 (2007).

Figures of merit in high-frequency and high-power GaN HEMTs

F. A. Marino, N. Faralli, D. K. Ferry, S. M. Goodnick and M. Saraniti

Department of Electrical Engineering, *Journal of Physics: Conference Series*, IOP Publishing, Arizona State University, 12 Tempe, AZ, 85287 USA

E-mail: Fabio.Marino@asu.edu

Abstract.

The most important metrics for the high-frequency and high-power performance of microwave transistors are the cut-off frequency f_T, and the *Johnson figure of merit* $FoM_{Johnson}$. We have simulated a state-of-the-art, high-frequency and high-power GaN HEMT using our full band Cellular Monte Carlo (CMC) simulator, in order to study the RF performance and compare different methods to obtain such metrics. The current gain as a function of the frequency, was so obtained both by the Fourier decomposition (FD) method and the analytical formula proposed by Akis. A cut-off frequency f_T of $150\ GHz$ was found in both the transit time analysis given by the analytical approach, and the transient Fourier analysis, which matches well with the $153\ GHz$ value measured experimentally. Furthermore, through some physical considerations, we derived the relation between the $FoM_{Johnson}$ as a function of the breakdown voltage, V_{BD}, and the cut-off frequency, f_T. Using this relation and assuming a breakdown voltage of $80V$ as measured experimentally, a Johnson figure of merit of around $20 \times 10^{12} V/s$ was found for the HEMT device analyzed in this work.

1. Introduction

Several figures of merit are often used to evaluate the performance of microwave devices. The most important metrics for the high-frequency and high-power performance of microwave transistors are the cut-off frequency, f_T, and the *Johnson figure of merit*, $FoM_{Johnson}$ [1]. The cut-off frequency is related to the short circuit current gain, h_{21}, which is defined as the ratio of the small-signal output current to the small-signal input current of the device when the output terminals are shorted. The Johnson figure of merit takes into account the breakdown electric field, E_{BD}, and saturated electron drift velocity, v_{sat}, in defining a measure for the power handling capability at high frequencies.

We have simulated a state-of-the-art, high-frequency and high-power GaN HEMT, reported by Palacios *et al.* [2], using our full band Cellular Monte Carlo (CMC) simulator, in order to study the RF performance and compare with the prediction of the analytical model for the cut-off frequency calculations proposed by Akis $et\ al.$ [3]. Furthermore, through some physical considerations, we derived the relation between the $FoM_{Johnson}$ in function of the breakdown voltage V_{BD} and the cut-off frequency f_T. Using this equation, the Johnson figure of merit can be connected directly to microwave measurements in a meaningful manner and calculated easily by standard experimental measurements.

2. GaN HEMT with InGaN back barrier

The layout of the device described in this work is composed of an $AlGaN/GaN$ heterostructure with an $InGaN$ back barrier grown on a semi-insulating SiC substrate by metal-organic chemical vapor

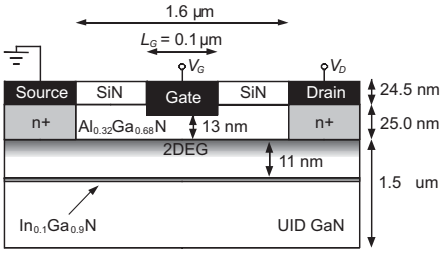

Figure 1. Schematic cross-section of the simulated InGaN back barrier HEMT

deposition. The heterostructure is unintentionally doped and consists, from bottom to top, of $1.5\mu m$ of GaN followed by $1nm$ of $In_{0.1}Ga_{0.9}N$ capped by $11nm$ of GaN and $25nm$ of $Al_{0.32}Ga_{0.64}N$ as shown in Figure 1. The $AlGaN$ layer is recessed in order to have a gate-to-channel distance of $13nm$. The source-gate and gate-drain separations are both $0.75\mu m$, while the gate length is set to $0.1\mu m$. Highly doped regions are created under the source-drain electrodes down to the GaN channel to emulate metal spikes and to control contact resistances.

The presence of the $InGaN$ layer enhances the confinement of the electrons in the channel. In fact, the large polarization-induced electric field in the $InGaN$ layer raises the conduction band edge of the GaN buffer with respect to the GaN channel, creating a potential barrier against carrier diffusion in the bulk layer. More details on that device can be found in [2], where all the characteristics of the sample used to obtain the experimental data are reported.

3. RF analysis of AlGaN/GaN HEMT

The basic idea of the small-signal frequency, or RF, analysis consists of applying a small perturbation to one electrode of the device in steady-state, while keeping all other parameters constant. The small-signal parameters can then be derived from the Fourier analysis of the transient response. The response in the transient regime is a function of the device characteristics, such as the geometry, the doping profile, the transport properties of the device and the steady-state operating point (i.e. the DC components of V_{DS} and V_{GS}).

In our study, the operating point for the RF analysis ($V_{GS} = 0V$, $V_{DS} = 6V$) has been chosen in order to compare simulation results with experiment [2]. The current gain as a function of the frequency is shown in Figure 2. The right plot, representing the simulation results, is obtained by the Fourier decomposition (FD) method, where a small step voltage is applied to the input port of the device in steady state, and the transient short circuit current response is Fourier analyzed to obtain the cut-off frequency.

4. Cut-off frequency

An alternative method to calculate the current gain cut-off frequency, f_T, is to relate this to the transient time at carriers across the effective gate length [3]:

$$f_T = \left[2\pi \int_{L_{eff}} \frac{1}{v_{ave}(x)} dx \right]^{-1}, \tag{1}$$

where L_{eff} is an effective gate length and $v_{ave}(x)$ is the average simulated velocity along the channel.

The simulated electron drift velocity profile along the channel used in the calculation of the cut-off frequency according to Eq. (1) is illustrated in Figure 3.

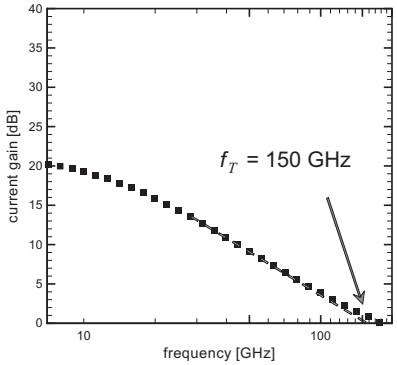

Figure 2. Current gain as a function of the frequency obtained by the CMC simulation.

A cut-off frequency f_T of $150\ GHz$ was found in both the transit time analysis given by Eq.(1), and simulation results using transient Fourier analysis, which matches well with the $153\ GHz$ value measured experimentally [2].

5. Johnson figure of merit

In general, widebandgap materials like GaN have desirable properties for high power applications due to their large band gap and high thermal conductivity. The Johnson figure of merit mentioned earlier, characterizes the high frequency performance of power devices, and is proportional to the saturation velocity and critical electric field for impact ionization initiated breakdown [1]

$$FoM_{Johnson} = \frac{v_{sat} E_{BD}}{2\pi}, \tag{2}$$

where v_{sat} is the saturation velocity and E_{BD} is the electric field at which impact ionization initiates breakdown. Unfortunately, this figure of merit is difficult to determine experimentally as both v_{sat} and E_{BD} are intrinsic properties of a device, although easily found from simulation. However, these quantities can be connected to microwave measurements in a meaningful manner. Generally, the cutoff frequency, f_T, is related to the effective saturation velocity through the well-known formula

$$f_T = \frac{v_{sat}}{2\pi L_G}, \tag{3}$$

where L_G is the gate length (or effective gate length). We also find from detailed simulations, that the field under the gate varies almost linearly over the length of the effective gate. Breakdown usually occurs near the drain end of the gate, where the highest field occurs. Since there is also a potential drop across the space between the gate and the contacts, we can write the breakdown voltage in terms of the breakdown field as

$$V_{BD} = \alpha \frac{E_{BD} L_G}{2} \tag{4}$$

where α is an adjustable parameter that relates the voltage drop across the gate to the total voltage applied to the device. Hence, we can rewrite the figure of merit in terms of these experimentally determined parameters as

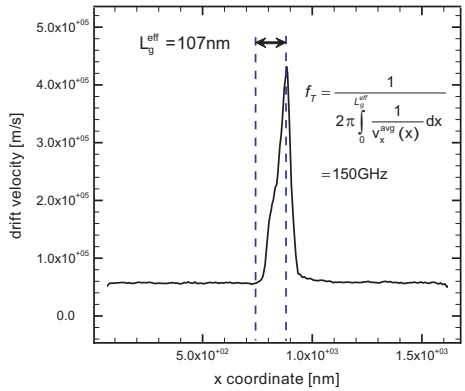

Figure 3. Electron drift velocity profile along the channel resulting by the CMC simulation

$$FoM_{Johnson} = \frac{1}{2\pi}(2\pi L_G f_T)\frac{2V_{BD}}{\alpha L_G} = \frac{2}{\alpha} f_T V_{BD}. \quad (5)$$

The α parameter can be extracted directly from the simulations using Eq. (4), and calculating the breakdown voltage as an integral of the field across the channel when the impact ionization first occurs.

Using a value previously published for GaN for Eq. (2) [4], and values found in simulations of GaN HEMTs, we find that α is appropriately 1.25, although this factor could be ignored without much loss of relevance of the figure of merit since its close to unity. Following Eq. (5) and assuming a breakdown voltage of 80V [2], a $FoM_{Johnson}$ around $20 \times 10^{12} V/s$ was found for the HEMT device analyzed in this work.

6. Conclusion

In this paper, the most important metrics to evaluate RF performance of GaN HEMT devices were investigated, through comparison between experimental, simulation and analytical method. The Fourier decomposition method was used to evaluate the cut-off frequency in our full band CMC simulation code, which includes the full details of the band structure and the phonon spectra. Thermal simulations were performed with commercial software in order to determine the corrections needed to model thermal effects with our particle-based CMC simulator. Our studies indicate that both the transit time analysis given by Eq.(1), and simulation results using transient Fourier analysis, matches well with the experimental data. We also derived an analytical model to determine the Johnson figure of merit and extracted this quantity from standard experimental data.

References

[1] A. Johnson, "Physical limitations on frequency and power parameters of transistors," *RCA Review*, vol. 26, pp. 163 – 177, 1965.

[2] T. Palacios, Y. Dora, A. Chakraborty, C. Sanabria, S. Keller, S. P. DenBaars, and U. K. Mishra, "Optimization of AlGaN/GaN HEMTs for high frequency operation," *Physica Status Solidi A*, vol. 203, no. 7, pp. 1845 – 1850, May 2006.

[3] R. Akis, J. Ayubi-Moak, N. Faralli, D. K. Ferry, S. M. Goodnick, and M. Saraniti, "The upper limit of the cutoff frequency in ultrashort gate-length InGaAs/InAlAs HEMTs: A new definition of effective gate length," *IEEE Electron Device Letters*, vol. 29, no. 4, pp. 306 – 308, April 2008.

[4] P. Das and D. Ferry, "Hot electron microwave conductivity of wide bandgap semiconductors," *Japanese Journal of Applied Physics*, vol. 19, pp. 851 – 855, 1976.

11th International Conference
on Advanced Materials

Rio de Janeiro Brazil
September 20 - 25

ICAM2009

Advanced Electron Microscopy Characterization of GaN-based High Electron Mobility Transistors

D. A. Cullen[(1)]*, L. Zhou[(2)], J. Leach[(3)], H. Morkoc[(3)], P. L. Fejes[(4)], D. J. Smith[(2)], and M. R. McCartney[(2)]

(1) School of Materials, Arizona State University, Tempe, AZ 85287-8706 USA
email: david.a.cullen@asu.edu
(2) Department of Physics, Arizona State University, Tempe, AZ 85287-1504 USA
(3) Department of Electrical Engineering, Virginia Commonwealth Univ, Richmond, VA 23284 USA
(4) Freescale Semiconductor Inc., 2100 E Elliot Rd, Tempe, AZ 85284 USA
* Corresponding author.

Abstract – Electron holography, scanning transmission electron microscopy (STEM), and energy-dispersive x-ray spectroscopy (EDX) have been used to characterize GaN-based high electron mobility transistor (HEMT) heterostructures and devices. Cross-sections prepared by the focused ion beam (FIB) lift-out and wedge-polish methods have been compared to determine the impact of ion-beam damage on phase imaging. Potential profiles and polarization fields within HEMT devices were measured by electron holography. Nanoscale chemical analysis was used to study the variations in electric fields between the device source and gate in terms of interdiffusion with contact and capping materials.

The AlGaN/GaN heterostructure provides the basis for the current generation of high electron mobility transistor (HEMT) devices [1]. In the case of III-nitride materials grown in the usual *c*-plane direction, spontaneous and piezoelectric polarization fields give rise to a two-dimensional electron gas (2-DEG) at the heterostructure interface. The presence of the 2-DEG leads to devices with high electron mobility that are suitable for high voltage, high frequency applications such as microwave communications and high power amplifiers [2]. This research focuses on the characterization of HEMTs by advanced electron microscopy methods including nanoscale chemical analysis and off-axis electron holography [3]. The investigation is broken into three subgroups: sample preparation using focused-ion-beam, off-axis holography to image electrostatic fields, and chemical and micro-structural analysis of devices.

Figure 1 shows an example of a HEMT device prepared by FIB for electron holography. Although the FIB is very useful for site-specific sample preparation, amorphization and implantation by the ion beam can easily alter the material structure. To determine the impact of FIB damage on phase imaging, both wedge and FIB samples were prepared from bulk HEMT heterostructures. Lorentz- and diffraction-mode electron holography was performed on both bulk and device samples. The potential profile across the heterostructure was calculated from the phase image using the relationship: $\Delta\phi = C_e t V$, where V is the potential, t is the sample thickness, and C_e is an energy-dependent interaction constant. Figure 2 shows the potential profile of a GaN/AlN/AlGaN heterostructure. The Pt capping layer was deposited as part of the FIB sample preparation. The 2-DEG is located on the substrate side of the GaN/AlN interface, as evidenced by the peaked region in the potential profile. High-angle annular-dark-field STEM imaging and EDX were used to qualitatively probe the chemical composition of these HEMT heterostructures. An EDX linescan across the channel of a HEMT device is show in Fig 3 [4].

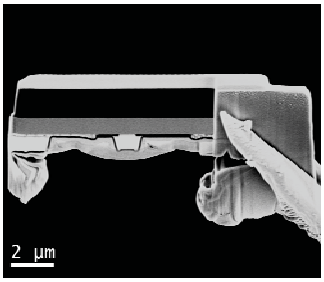

Figure 1: SEM image of HEMT device prepared by FIB lift-out method.

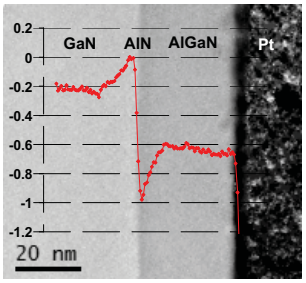

Figure 2: Phase image of GaN/AlN/AlGaN heterostucture obtained by holography with calculated potential profile (overlay).

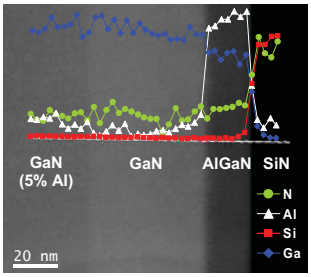

Figure 3: STEM image of HEMT device with EDX linescan profiles (overlay).

[1] O. Ambacher et al., *J. Appl. Phys.* 85 (1999) 3222-3233.
[2] U.K. Mishra et al., *Proc. IEEE* 96 (2008) 287-305.
[3] M.R. McCartney et al., *J. Appl. Phys.* 82 (1997) 2461-2465.
[4] This work was supported by a contract from Wright-Patterson Air Force Base (Monitor: C. Bozada). We gratefully acknowledge the use of facilities within the John M. Cowley Center for High Resolution Electron Microscopy at Arizona State University.